Journal of Biomechanics xxx (2018) xxx–xxx

Contents lists available at ScienceDirect

Journal of Biomechanics

journal homepage: www.elsevier.com/locate/jbiomech
www.JBiomech.com

Short communication

Experimental evaluation of current and novel approximations of articular surfaces of the ankle joint

Claudio Belvedere [a,*], Sorin Siegler [b], Andrea Ensini [c], Jason Toy [b], Paolo Caravaggi [a], Ramya Namani [b], Luca Giuseppe Princi [a], Stefano Durante [d], Alberto Leardini [a]

[a] Movement Analysis Laboratory, IRCCS Istituto Ortopedico Rizzoli, Bologna, Italy
[b] Department of Mechanical Engineering and Mechanics, Drexel University, Philadelphia, PA, USA
[c] 1st Orthopedic-Traumatologic Clinic, IRCCS Istituto Ortopedico Rizzoli, Bologna, Italy
[d] Nursing, Technical and Rehabilitation Assistance Service, IRCCS Istituto Ortopedico Rizzoli, Bologna, Italy

ARTICLE INFO

Article history:
Accepted 14 April 2018
Available online xxxx

Keywords:
Ankle
Replacement
Morphology
Articular surfaces
Kinematics
Flexibility
In-vitro

ABSTRACT

Kinematics and flexibility properties of both natural and replaced ankle joints are affected by the geometry of the articulating surfaces. Recent studies proposed an original saddle-shaped, skewed, truncated cone with laterally oriented apex, as tibiotalar contact surfaces for ankle prosthesis. The goal of this study was to compare *in vitro* this novel design with traditional cylindrical or medially centered conic geometries in terms of their ability to replicate the natural ankle joint mechanics. Ten lower limb cadaver specimens underwent a validated process of custom design for the replacement of the natural ankle joint. The process included medical imaging, 3D modeling and printing of implantable sets of artificial articular surfaces based on these three geometries. Kinematics and flexibility of the overall ankle complex, along with the separate ankle and subtalar joints, were measured under cyclic loading. In the neutral and in maximum plantarflexion positions, the range of motion under torques in the three anatomical planes of the three custom artificial surfaces was not significantly different from that of the natural surfaces. In maximum dorsiflexion the difference was significant for all three artificial surfaces at the ankle complex, and only for the cylindrical and medially centered conic geometries at the tibiotalar joint. Natural joint flexibility was restored by the artificial surfaces nearly in all positions. The present study provides experimental support for designing articular surfaces matching the specific morphology of the ankle to be replace, and lays the foundations of the overall process for designing and manufacturing patient-specific total ankle replacements.

1. Introduction

Total ankle replacement (TAR) is frequently performed for the treatment of end-stage ankle osteoarthritis. Unlike total hip and knee joint replacements, this treatment still suffers from high failure rates and clinical complications, in addition to low patient's satisfaction (Bartel and Roukis, 2015; Spirt et al., 2004). The ability to reproduce the original natural mobility and stability of the ankle joint complex with TAR has been recognized as a key factor for the clinical success of this surgical treatment (Giannini et al., 2010; Leardini et al., 2004). In more mechanical terms, the goal of TAR is to replicate the original range and pattern of rotations, hereinafter referred to as kinematics, and also the original rotational response to external torques, hereinafter referred to as flexibility (or laxity as in Belvedere et al., 2017). Because morphology and function at the ankle joint are complex (Leardini et al., 1999; Lundberg et al., 1989; Siegler et al., 1988), a major TAR design challenge is to produce artificial articular surfaces that best approximate morphology to possibly restore function, as observed in the intact ankle. Original studies on functional morphology of the ankle (Close, 1956; Hicks, 1953; Barnett and Napier, 1952; Close and Inman, 1952) established a single fixed axis of rotation at the tibiotalar joint, and a cylindrical or conical approximation for the talar dome, the latter having the apex on the medial side of the joint (Inman, 1976; Close and Inman, 1952). A recent image-based 3D study showed that the trochlear surface of the talus, and the articulating distal tibial surface, can be approximated by a saddle-shaped skewed truncated cone with laterally oriented apex (SSCL) (Siegler et al., 2014). This was recently supported by experimental evidence *in vitro* (Belvedere et al., 2017). Different

* Corresponding author at: Movement Analysis Laboratory, IRCCS Istituto Ortopedico Rizzoli, Via di Barbiano 1/10, Bologna, Italy.
E-mail address: belvedere@ior.it (C. Belvedere).

https://doi.org/10.1016/j.jbiomech.2018.04.024
0021-9290/

geometrical approximations of the artificial articular surfaces of TAR designs would result in different kinematics and flexibility at the replaced ankle, and, in the long term, in different clinical outcomes.

A previous paper from the present authors (Belvedere et al., 2017) has established the reliability of an experimental *in vitro* procedure to assess TAR implants, and the performance of the SSCL surfaces. The goal of the present study was to use this technique to compare the effect, in terms of kinematics and flexibility at the replaced ankle, of three possible different articular surfaces: the SSCL, a cylindrical, and a conical with apex oriented medially. The latter two are used in the large majority of the current TAR designs. For this purpose, custom 3D-printed implants, based on the three concepts mentioned above, were originally produced from 3D computer models of articulating bones.

2. Materials and methods

The overall procedures for implants design and manufacturing, experimental set-up and protocol, specimens population, and most of the data analysis have been previously reported (Belvedere et al., 2017). Briefly, ten cadaver legs disarticulated at the knee were defrosted at room temperature, and relevant radiographic images and surgeon inspections excluded ankle deformities or instability and cartilage defects. For each specimen, computer-tomography scans were processed (Analyze Direct™, Overland Park, KS-USA) to obtain 3D models of the tibia, fibula, talus and calcaneus. These were further processed (Geomagic™, Morrisville, NC-USA) to extract specimen-specific design parameters required to produce three different artificial surface approximations of the natural joint surfaces, as follow (Fig. 1): SSCL, matching saddle-shaped truncated cones with laterally oriented apex resulting from subject-specific anatomy (Belvedere et al., 2017; Siegler et al., 2014); cylindrical (CYL), matching cylindrical surfaces with the talar dome radius being the average between the radii of the relevant medial and lateral crest contours; and truncated-cone with a fixed medially-oriented apex (TCM) as claimed by Inman (1976). The final design of these three implants, consisting each of a tibial and a talar component, was performed using Inventor™ (AutoDesk, San Rafael, CA-USA). CYL and TCM are meant to represent the articulating geometry of most current TAR designs (Kakkar and Siddique, 2011; Lewis, 1994). The components were fixed to the bone via screws in their frontal aspect. At the distal tibia, two parallel tunnels drilled from the front were used as references to register bone models and the implants. The three implants were 3D-printed (Dimensions Elite™ by Stratasys, Inc.; nominal spatial resolution 0.2 mm) in acrylonitrile-butadienestyrene.

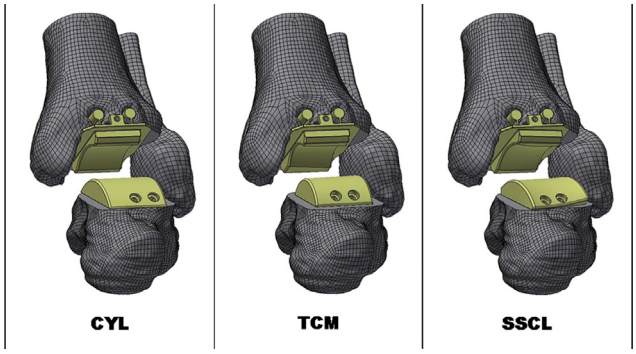

Fig. 1. Model rendering from the analysis of one typical specimen, after the design of the three implant sets: cylindrical-CYL (left), truncated-cone with medial apex – TCM (centre), and saddle shaped skewed truncated cone with laterally oriented apex – SSCL (right). The replaced joint is separated just to illustrate better the artificial surfaces.

Following surgical preparation of the specimen (Belvedere et al., 2017), each implant set was inserted, one at a time, and secured to the corresponding bone. Before and after each implantation, tests were performed to determine their corresponding mechanical response under these four conditions: with the natural surfaces (NATURAL), and following the replacement of the natural surfaces with the CYL, TCM, and SSCL implants. For this purpose, an Ankle Flexibility Tester (AFT, (Belvedere et al., 2017; Siegler et al., 1996)), and an optoelectronic stereo-photogrammetric system (Stryker Knee Navigation System, Stryker®, Kalamazoo, MI-USA (Belvedere et al., 2014)) were used. This whole experimental setup was able to apply and measure continuous torque across the ankle complex while measuring motion at the ankle, subtalar, and ankle complex joints, by tracking motion of the tibia, talus, and calcaneus. A 6 degree-of-freedom tracker was pinned to each bone to measure 3D kinematics. A fourth tracker was used for system control and anatomical landmark digitization.

Passive motion was first tracked over the entire range of flexion/extension without the use of the torque sensor because of the large flexibility in this rotational direction. Subsequently, the torque sensor was used to manually apply and measure torque about the inversion/eversion and internal/external rotation axes of the AFT (Siegler et al., 1996). These torques were applied starting from three different joint positions within the full flexion arc: neutral (Neutral); maximum dorsiflexion (MaxDorsi), and maximum plantarflexion (MaxPlantar). The torques applied, measured and reported were those just required to reach the end of the range of motion in each condition. These tests were repeated for at least four loading-unloading cycles and replicated for the four joint conditions.

After testing the ankle in NATURAL, with the specimen still secured to the AFT, the surgeon used a standard surgical instrumentation for TAR (Giannini et al., 2010) to prepare the bone for the implantation, one at time, of each of the three implants. The tibiotalar articular surfaces were exposed by a standard anterior surgical approach. Bone preparation was performed by saws and drills with the support of the tibial jig. The CYL, TCM and SSCL implants were then tested. At the end, digitization of fiduciary markers for registration and of anatomical landmark for coordinate frame definitions (Cappozzo et al., 1995) was performed by using the ad-hoc optoelectronic tracker. For the latter, an established joint coordinate system convention (Grood and Suntay, 1983) was used to calculate dorsiflexion/plantarflexion (Dor-Pla), inversion/eversion (Inv-Eve) and internal/external rotation (Int-Ext), at the ankle, subtalar, and ankle complex joints.

For each specimen, each joint condition, each mechanical test and each repetition, collected data were first normalized to 0–100% of each passive or loading-unloading cycle. In order to isolate the effect of the artificial articular surfaces, differences between CYL, TCM and SSCL and the NATURAL conditions were calculated for each mechanical variable along the cycle. In addition, overall flexibility values were also obtained, here defined as the ratio between the total range of motion measured in the torque cycle and the corresponding maximum joint torque. These were tested for statistical significance as differences between intact and replaced joint conditions, using repeated-measure multifactor analysis of variance with a significance value of $p < 0.05$.

3. Results

Intra specimen repeatability, measured as the standard deviation of the repetitions, was smaller than 2.0 deg and 0.3 N m for joint rotation and flexibility, respectively (Belvedere et al., 2017).

Please cite this article in press as: Belvedere, C., et al. Experimental evaluation of current and novel approximations of articular surfaces of the ankle joint. J. Biomech. (2018), https://doi.org/10.1016/j.jbiomech.2018.04.024

In absolute terms, all three artificial surfaces reproduced original natural rotation in the same direction (Fig. 2). In passive flexion, nearly the same range of motion was achieved at the ankle and ankle complex joints (respectively 40.6 ± 8.2 and 39.3 ± 7.3 deg as averaged over the specimens at the NATURAL joint), with limited dorsiflexion at subtalar joint (2.9 ± 1.9 deg). Under both inversion/eversion and internal/external torques (respectively 11.4 ± 0.6 and 9.6 ± 0.8 N/m as averaged over the specimens at the NATURAL joint), the largest range of primary motion, i.e. in the same direction of the torque applied at the ankle joint complex, was found in MaxPlantar position (respectively 18.4 ± 6.1 and 28.6 ± 4.7 deg at the NATURAL joint), the smallest in MaxDorsi (respectively 9.1 ± 3.5 and 12.9 ± 6.0 deg), likely because of the corresponding increasing conformity between the tibial mortise and the talus.

To point out variations associated to three implant sets, artificial-to-natural differences in joint rotation over full torque

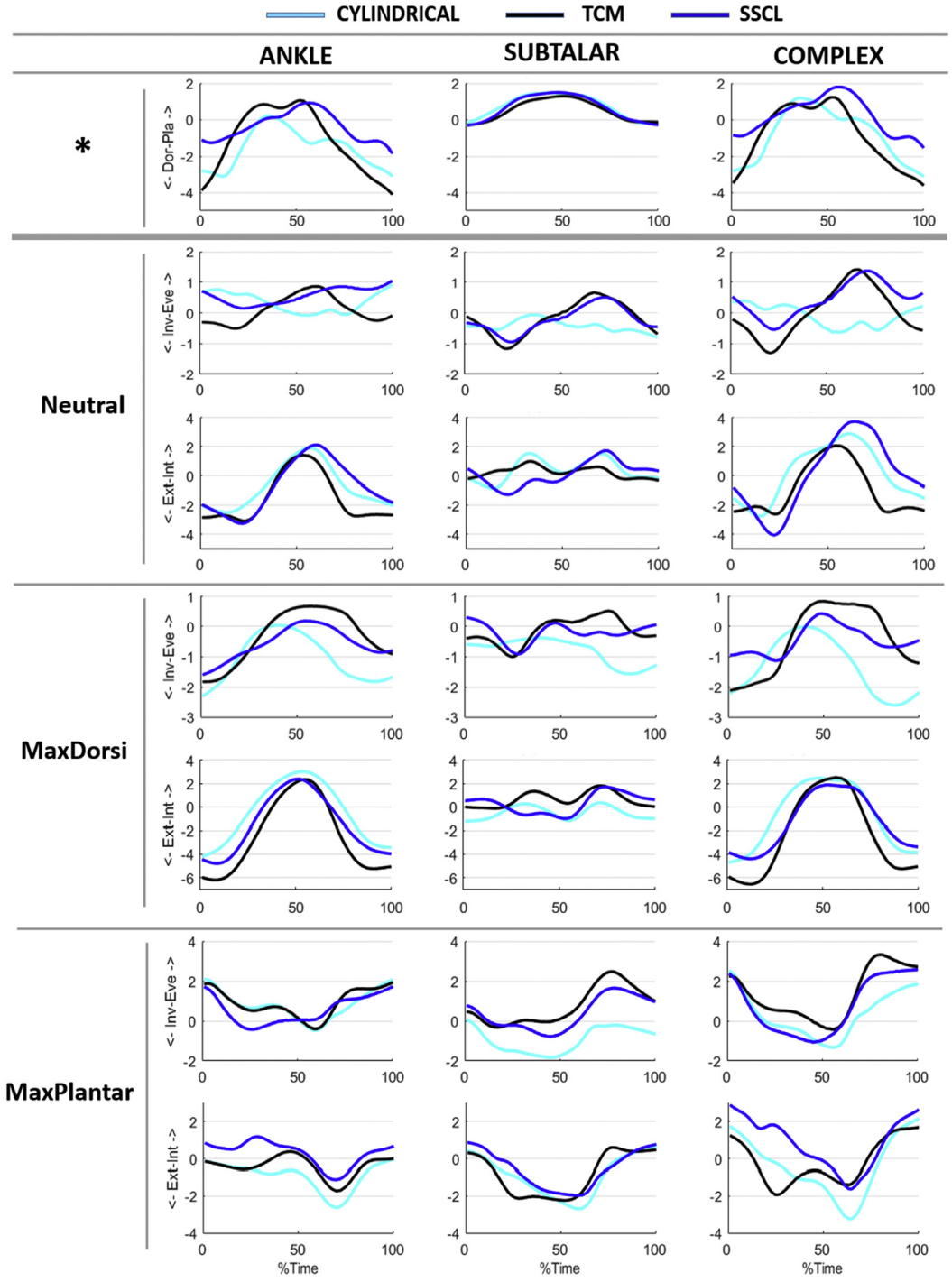

Fig. 2. Inter-specimen average of the difference in joint rotation patterns between NATURAL and the three artificial sets CYL (cyan), TCM (black) and SSCL (blue) over the normalized (0–100%) loading-unloading cycle duration. Temporal patterns are reported for the ankle, subtalar, and ankle complex joints. Dorsiflexion-Plantarflexion (Dor-Pla) is reported for the full range of flexion (* no torque sensor used in this direction); joint motion produced through torque application in inversion-eversion (Inv-Eve) and internal-external rotation (Int-Ext) are also reported; finally, flexions started from the Neutral, maximum dorsiflexion (MaxDorsi) and maximum plantarflexion (MaxPlantar) joint positions are reported. (For interpretation of the references to colour in this figure legend, the reader is referred to the web version of this article.)

Please cite this article in press as: Belvedere, C., et al. Experimental evaluation of current and novel approximations of articular surfaces of the ankle joint. J. Biomech. (2018), https://doi.org/10.1016/j.jbiomech.2018.04.024

cycles are shown in Fig. 2, and these are expressed in Table 1 in terms of peak-to-peak differences along with the corresponding maximum torque applied. Interestingly, in passive flexion the TCM implants showed significant differences at the subtalar and ankle joints, but not at the ankle complex (Table 1). In Neutral and MaxPlantar joint positions no significant differences were observed. In MaxDorsi, the range of motion was significant larger for all three artificial surfaces at the ankle complex under internal/external rotation torques. Under inversion/eversion and internal/external rotation torques, differences only for the CYL and TCM implants were found significant at the ankle joint.

In terms of total flexibility (Table 2), SSCL showed no significant differences compared to the natural joint, whereas one significant difference was found for the TCM and two for the CYL.

The design parameters confirmed the original lateral location of the pivot point in the SSCL approach. This can be deduced by the observed difference between the medial and the lateral radii of the talar dome (2.7 ± 1.2 mm, range 0.8–5.5). Large differences were observed in the coronal view of the top of the central talar dome, here measured by the relevant radius of the best fit circle (49.4 ± 28.8 mm, range 20.5–100.9). These two parameters represent the major features of this original skewed-cone based design, respectively the direction of the cone, opposite as expected to what it was believed for decades, and the characterization of the typical saddle-shape.

4. Discussion

The unsatisfactory clinical results of TAR may be partially associated with the current prosthesis designs, particularly the shape of the articulating surfaces which largely contribute to kinematics and flexibility of the replaced ankle (Franci et al., 2009; Leardini et al., 2004; Leardini et al., 1999). In addition, the small number of available sizes for TAR systems, due mainly to the limited indication for this treatment, hinders the perfect component-to-bone

Table 1
Primary kinematics and torques, in [degrees] and [N*m] respectively, at the ankle, subtalar and complex joints. Dorsiflexion-Plantarflexion (Dor-Pla) is reported for the full range of flexion (* no torque sensor used in this direction). Range of motion produced through torque application in inversion-eversion (Inv-Eve) and internal-external rotation (Int-Ext) starting from the Neutral, maximum dorsiflexion (MaxDorsi) and maximum plantarflexion (MaxPlantar) joint positions are reported for the ankle, subtalar, and ankle complex joints as mean ± standard deviations over specimens; p-values are also reported in brackets (p=) only for the statistically significant comparisons, i.e. those with $p < 0.05$. In the three columns, the difference in range of motion between the NATURAL and the CYL ($\Delta_{CYL\text{-}NAT}$), TCM ($\Delta_{TCM\text{-}NAT}$) and SSCL ($\Delta_{SSCL\text{-}NAT}$) artificial sets of articular surfaces are reported. The corresponding differences in the torque applied (rows TORQUE) are also reported.

			$\Delta_{CYL\text{-}NAT}$ mean ± SD	$\Delta_{TCM\text{-}NAT}$ mean ± SD)	$\Delta_{SSCL\text{-}NAT}$ mean ± SD
*	Dor – Pla	ANKLE	1.3 ± 3.7	3.9 ± 5.0 (p = 0.0331)	1.1 ± 5.4
		SUBTALAR	−0.7 ± 1.6	−0.9 ± 0.9 (p = 0.0401)	−0.5 ± 1.6
		COMPLEX	2.7 ± 5.4	3.6 ± 4.9	1.7 ± 4.7
Neutral	Inv – Eve	ANKLE	1.9 ± 4.6	2.7 ± 3.9	1.8 ± 4.0
		SUBTALAR	0.3 ± 5.1	0.4 ± 4.6	0.5 ± 4.6
		COMPLEX	0.3 ± 7.9	1.7 ± 7.9	0.7 ± 7.2
		TORQUE	−0.6 ± 1.7	−0.3 ± 1.1	−0.3 ± 0.9
	Ext – Int	ANKLE	3.6 ± 5.8	4.2 ± 6.0	3.1 ± 7.4
		SUBTALAR	0.6 ± 3.1	0.1 ± 4.0	−1.0 ± 4.5
		COMPLEX	3.6 ± 7.4	4.4 ± 6.4	2.4 ± 6.2
		TORQUE	−0.5 ± 1.5	−0–5 ± 1.3	−0.8 ± 1.5
MaxDorsi	Inv – Eve	ANKLE	2.5 ± 2.1 (p = 0.0185)	3.6 ± 2.3 (p = 0.0062)	1.7 ± 1.8
		SUBTALAR	0.7 ± 3.7	0.8 ± 4.6	−0.3 ± 4.1
		COMPLEX	3.1 ± 5.6	4.0 ± 6.8	1.8 ± 5.9
		TORQUE	−0.3 ± 1.1	−0.8 ± 1.9	−0.3 ± 1.6
	Ext – Int	ANKLE	7.0 ± 4.0 (p = 0.0037)	7.7 ± 3.5 (p = 0.0012)	6.5 ± 6.5
		SUBTALAR	−0.7 ± 4.5	−0.7 ± 5.3	−1.6 ± 4.7
		COMPLEX	6.8 ± 2.7 (p = 0.0005)	7.7 ± 2.5 (p = 0.0002)	5.4 ± 4.5 (p = 0.0194)
		TORQUE	−0.6 ± 2.6	−1.4 ± 1.6	−1.1 ± 1.8
MaxPlantar	Inv – Eve	ANKLE	1.5 ± 4.8	2.7 ± 5.8	1.7 ± 5.1
		SUBTALAR	−1.2 ± 3.9	−0.8 ± 3.6	−1.4 ± 4.2
		COMPLEX	−1.9 ± 5.0	−0.7 ± 3.9	−2.3 ± 3.4
		TORQUE	0.3 ± 1.7	0.6 ± 1.7	0.7 ± 0.9
	Ext – Int	ANKLE	−1.0 ± 7.9	0.1 ± 6.8	−0.6 ± 6.4
		SUBTALAR	−3.0 ± 5.4	−2.7 ± 5.3	−2.9 ± 5.5
		COMPLEX	−3.9 ± 6.4	−2.6 ± 6.8	−3.3 ± 6.3
		TORQUE	−0.3 ± 1.0	−0.7 ± 1.7	−0.1 ± 1.5

Table 2
Primary total flexibility in [degrees/(N*m)] of the ankle complex in inversion/eversion and internal/external rotation. Data are reported as mean ± standard deviations over specimens; p-values are also reported in brackets (p=) only for the statistically significant comparisons, i.e. those with $p < 0.05$. In the three columns the difference in total flexibility between NATURAL joint and the CYL ($\Delta_{CYL\text{-}NAT}$), TCM ($\Delta_{TCM\text{-}NAT}$) and SSCL ($\Delta_{SSCL\text{-}NAT}$) artificial sets of articular surfaces are reported.

		$\Delta_{CYL\text{-}NAT}$ mean ± SD	$\Delta_{TCM\text{-}NAT}$ mean ± SD	$\Delta_{SSCL\text{-}NAT}$ mean ± SD
Neutral	Inv – Eve	0.1 ± 0.8	0.3 ± 0.8	0.2 ± 0.8
	Ext – Int	1.0 ± 2.1	1.2 ± 1.8	1.5 ± 1.4
MaxDorsi	Inv – Eve	0.3 ± 0.6	0.5 ± 0.6	0.2 ± 0.6
	Ext – Int	1.1 ± 0.9 (p = 0.0310)	1.5 ± 0.8 (p = 0.0120)	0.9 ± 1.1
MaxPlantar	Inv – Eve	−0.4 ± 0.3 (p = 0.0101)	−0.3 ± 0.5	−0.6 ± 0.5
	Ext – Int	−0.3 ± 1.1	−0.2 ± 1.3	−0.5 ± 1.1

Please cite this article in press as: Belvedere, C., et al. Experimental evaluation of current and novel approximations of articular surfaces of the ankle joint. J. Biomech. (2018), https://doi.org/10.1016/j.jbiomech.2018.04.024

match, and therefore the short- and long-term fixation of the implants. In order to perform an isolate analysis of the effect of the articular surfaces, a possible new geometry, along with standard shapes, were tested in the present study in a number of ankle specimens, after careful customization of these surfaces. These preliminary tests *in vitro*, including kinematics and torque measurements, are in fact necessary before relevant long-term clinical studies can be planned. Following a previous paper from the present authors (Belvedere et al., 2017), where the SSCL surfaces and the overall procedure for imaging-processing-modeling-designing-manufacturing were introduced and validated, the present work reports on the exact comparison, in terms of kinematics and flexibility, between these novel surfaces and those more traditional in TAR, i.e. TCM and CYC. Originally, all these three implant sets were designed to match the specific morphology of each tested specimens, according to the corresponding designing approach. Therefore this study may also represent a demonstration case for possible future processes of TAR designing and manufacturing on a patient-specific basis.

The results of this study demonstrated an overall good restoration of the natural ankle joint mechanics for all three implants; CYL, TCM and SSCL sets presented respectively only 5, 6 and 1 significant differences (on aggregate from Tables 1 and 2) with respect to the kinematics and flexibility of the natural joint. This was particularly true in MaxDorsi, likely a consequence of the large congruency between articular surfaces at this extreme joint position which increases the relevant contribution of the surface geometry.

The present study is limited by the sample size and by some flaws in the testing setup, such as the roughness of the 3D-printed artificial surfaces and the lack of axial compressive loading. The results are also restricted to the present summarizing definition of joint flexibility, i.e. the ratio between range of motion and corresponding maximum torque (Table 2). Plots showing the entire course of torque-rotation curves, which would be a more comprehensive mechanical characterization of the natural and replaced ankle joints, in fact by did not reveal additional relevant information. In addition, the experimental analysis was performed on natural ankles only, and these may not provide the same biomechanical conditions present in the arthritic joints of patients undergoing ankle joint replacement. Rather, a strength of these measurements is in fact the exact customization of each implant set and the analysis of passive motion, which both contribute to isolate the unique effect of the articulating surfaces in the replaced ankle.

Overall, the outcome of the present investigation and of previous results (Belvedere et al., 2017) demonstrate that replacing the natural ankle joint by custom surfaces in the shape of a saddle skewed truncated cone with laterally oriented apex (Siegler et al., 2014) produces mobility and stability not worse than those obtained by surfaces mimicking traditional TAR designs, i.e. cylindrical and medially oriented truncated cone.

Acknowledgments

This study was support by a grant from the Coulter-Drexel Translational Research Partnership, Philadelphia (PA, USA), by the Italian Ministry of Economy and Finance within the program "5 per mille", and by Regione Emilia-Romagna (Italy), program POR-FESR Project 726346 – Custom-implants.

Conflict of interest statement

All authors declare that there are no personal or commercial relationships related to this work that would lead to a conflict of interest. Furthermore, local institutional review board approval is not required for this sort of studies.

References

Barnett, C.H., Napier, J.R., 1952. The axis of rotation at the ankle joint in man; its influence upon the form of the talus and the mobility of the fibula. J. Anat. 86 (1), 1–9.

Bartel, A.F., Roukis, T.S., 2015. Total ankle replacement survival rates based on Kaplan-Meier survival analysis of national joint registry data. Clin. Podiatr. Med. Surg. 32 (4), 483–494.

Belvedere, C., Ensini, A., Leardini, A., Dedda, V., Feliciangeli, A., Cenni, F., Timoncini, A., Barbadoro, P., Giannini, S., 2014. Tibio-femoral and patello-femoral joint kinematics during navigated total knee arthroplasty with patellar resurfacing. Knee. Surg. Sports Traumatol. Arthrosc. 22 (8), 1719–1727.

Belvedere, C., Siegler, S., Ensini, A., Toy, J., Caravaggi, P., Namani, R., Giannini, S., Durante, S., Leardini, A., 2017. Experimental evaluation of a new morphological approximation of the articular surfaces of the ankle joint. J. Biomech. 53 (2), 97–104.

Cappozzo, A., Catani, F., Croce, U.D., Leardini, A., 1995. Position and orientation in space of bones during movement: anatomical frame definition and determination. Clin. Biomech. (Bristol., Avon.) 10 (4), 171–178.

Close, J.R., 1956. Some applications of the functional anatomy of the ankle joint. J. Bone Joint Surg. Am. 38- A (4), 761–781.

Close, J.R., Inman, V.T., 1952. The Action of the Ankle Joint. Prosthetic Devices Research Project, Institute of Engineering Research. University of California, Berkeley.

Franci, R., Parenti-Castelli, V., Belvedere, C., Leardini, A., 2009. A new one-DOF fully parallel mechanism for modelling passive motion at the human tibiotalar joint. J. Biomech. 42 (10), 1403–1408.

Giannini, S., Romagnoli, M., O'Connor, J.J., Malerba, F., Leardini, A., 2010. Total ankle replacement compatible with ligament function produces mobility, good clinical scores, and low complication rates: an early clinical assessment. Clin. Orthop. Relat. Res. 468 (10), 2746–2753.

Grood, E.S., Suntay, W.J., 1983. A joint coordinate system for the clinical description of three-dimensional motions: application to the knee. J. Biomech. Eng. 105 (2), 136–144.

Hicks, J.H., 1953. The mechanics of the foot. I. The joints. J. Anat. 87 (4), 345–357.

Inman, V.T., 1976. The Joints of the Ankle. Williams & Wilkins, Baltimore.

Kakkar, R., Siddique, M.S., 2011. Stresses in the ankle joint and total ankle replacement design. Foot Ankle Surg. 17 (2), 58–63.

Leardini, A., O'Connor, J.J., Catani, F., Giannini, S., 1999. Kinematics of the human ankle complex in passive flexion; a single degree of freedom system. J. Biomech. 32 (2), 111–118.

Leardini, A., O'Connor, J.J., Catani, F., Giannini, S., 2004. Mobility of the human ankle and the design of total ankle replacement. Clin. Orthop. Relat. Res. 424, 39–46.

Lewis, G., 1994. The ankle joint prosthetic replacement: clinical performance and research challenges. Foot Ankle Int. 15 (9), 471–476.

Lundberg, A., Svensson, O.K., Nemeth, G., Selvik, G., 1989. The axis of rotation of the ankle joint. J. Bone Joint Surg. Br. 71 (1), 94–99.

Siegler, S., Chen, J., Schneck, C.D., 1988. The three-dimensional kinematics and flexibility characteristics of the human ankle and subtalar joints–Part I: Kinematics. J. Biomech. Eng. 110 (4), 364–373.

Siegler, S., Lapointe, S., Nobilini, R., Berman, A.T., 1996. A six-degrees-of-freedom instrumented linkage for measuring the flexibility characteristics of the ankle joint complex. J. Biomech. 29 (7), 943–947.

Siegler, S., Toy, J., Seale, D., Pedowitz, D., 2014. The clinical biomechanics award 2013 presented by the international society of biomechanics: new observations on the morphology of the talar dome and its relationship to ankle kinematics. Clin. Biomech. (Bristol., Avon.) 29 (1), 1–6.

Spirt, A.A., Assal, M., Hansen Jr., S.T., 2004. Complications and failure after total ankle arthroplasty. J. Bone Joint Surg. Am. 86-A (6), 1172–1178.